Engineering Failure Analysis 125 (2021) 105368

Contents lists available at ScienceDirect

Engineering Failure Analysis

journal homepage: www.elsevier.com/locate/engfailanal

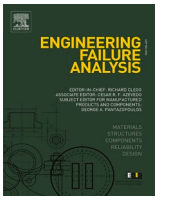

Probabilistic framework for failure investigation of reinforced concrete wall panel under dynamic blast loads

Tathagata Roy, Vasant Matsagar *

Multi-Hazard Protective Structures (MHPS) Laboratory, Department of Civil Engineering, Indian Institute of Technology (IIT) Delhi, Hauz Khas, New Delhi 110 016, India

ARTICLE INFO

Keywords:
Blast load
Fragility
RC wall panel
Sensitivity
Stochastic

ABSTRACT

Over the last decade, excessive devastations caused by extreme events, such as blast loading have raised significant concern on the performance of civil structural systems. Despite realizing the importance of inherent risk associated with this phenomenon, most of the studies neglected the effects of uncertainties associated with the system, wherein the design approaches have been entirely on deterministic scale. Hence, it is deemed important to identify the complexities in the system, and in this regard, a probabilistic framework is proposed which utilizes the effects of uncertainties in the system to compute the failure probabilities of a reinforced concrete (RC) structural member under extreme blast loading. The structural member adopted here is a three-dimensional (3-D) RC wall panel, which is modeled considering material and geometric nonlinearity, and the subsequent analysis is carried out under surface-burst and free airburst scenarios. High strain rate effect induced in the RC wall is modeled using available standard dynamic increase factors (DIFs) for concrete and steel. Uncertainty in the system is assumed in material capacity (strength), mechanical loads, and dynamic blast loads considering a certain mean and standard deviation. Responses are obtained in terms of deflection, stresses, and strains at center of the wall. Limit state of failure and the respective threshold limiting values are obtained from the United States Department of Defense manual, PDC-TR 06-08 (2008). Finally, first-order sensitivity analysis is conducted to show the extent of uncertainties in input parameters affecting the output response quantities. It is concluded that the uncertainty induced in the system has significant influence in the response of the wall panels under blast loading scenarios. Moreover, based on the sensitivity analysis performed, charge weight, standoff distance, and strength of concrete material are suggested to be crucial parameters for design of blast-resistant structures. To conclude, based on the currently considered scenario of intensity of blast, exposure type, and performance level required by the user, it is recommended to use wall panels of sizes more than 100 mm in civil structures, especially 125 mm to counter the effects of extreme blast loadings.

1. Introduction

Over the past two decades, excessive devastations caused by extreme events, such as blast loading have raised significant concern on the performance of civil structural systems [8]. Recent terrorist activities in the past half-decade (2013–2018) showed that more than 25 extreme terror incidents happened in India, which caused significant devastations to military camps as well as civil structures

* Corresponding author.
E-mail addresses: tathagata.roy@civil.iitd.ac.in (T. Roy), matsagar@civil.iitd.ac.in (V. Matsagar).

https://doi.org/10.1016/j.engfailanal.2021.105368
Received 12 October 2020; Received in revised form 17 February 2021; Accepted 11 March 2021
Available online 16 March 2021

and infrastructure systems. The attacks injured more than 340 people and killed more than 200 people, which included militants as well as civilians. Moreover, more than 20% of the attacks involved detonations, targeting civil and commercial structures. Therefore, these critical numbers illustrate the need of blast-resistant design for civil structures of general applications. Although economical restraints prevent the design of commercial structures to resist extreme loadings such as, explosive blast, the devastating effects clearly demonstrate the need for investigation of such civil structures along with military or other high-risk structures under extreme blast loading scenarios [23].

Reinforced concrete (RC) is a common and extensively used construction material for civil and commercial, military and strategic, and many important structures in India as well as in other different parts of the world. One of the most important advantages of RC material is that RC members require relatively lesser degree of treatment to achieve significant performance during accidental/ manmade disasters as compared to steel members. To utilize this advantage, reinforced concrete (RC) wall panels are mostly used in residential and commercial buildings. Moreover, the RC panels constitute of about 40%−60% of the total dead load of an ordinary RC building [60]. More importantly, apart from transferring and resisting loads, an RC wall panel also forms a part of building envelop, which is also expected to act as an insulation barrier to prevent heat loss and heat gain, in case of any accidental fire loads [43]. Hence, RC panels form an integral part of a building system and, therefore, it is deemed important to study the performance of the RC wall panels under extreme blast and explosion loads.

The traditional blast-resistant analysis and design was a simplistic approach, in which the structures were approximated as single-degree of freedom (S-DOF) systems [26,27,38,34,58,9,18]. Since then, the adopted S-DOF approach has been widely used in common blast-resistant design standards [58,59]; however, this approach overestimates the design values, not essentially leading to accurate estimation of structural response. Thereafter, experimental tests and numerical simulations were required to quantify the structural responses more accurately [63,3,21,39]. As wall panels form the building envelope and first line of defense against any accidental blast or explosion events, the analysis and design approaches were more inclined towards blast-resistant design. Researches on blast-resistant design of panel members involved the use of different innovative materials such as, carbon fiber and steel fiber reinforced polymers, aluminum cenosphere syntactic foam (ACSF), steel stiffeners, aluminum alloy foam, precast plates, etc. [50,15,61,31]. The investigations showed that the use of these materials provided a relatively higher degree of blast resistance. Furthermore, Yao et al. [64] conducted experimental and numerical studies to investigate the behavior and damage patterns of RC slabs under blast loadings. As anti-terrorism design guidelines, they demonstrated that the deflection to thickness ratio of the RC slab member is inversely proportional to scaled distance and ratio of shear reinforcement. Recent critical study conducted by Goswami and Adhikary [17] highlighted the use of 'mixed retrofitting' scheme to achieve higher energy absorption under blast loading. Lately, Abbas et al. [2] conducted experimental investigation to assess the behavior of reinforced concrete sandwiched panels (RCSPs) under free airburst scenario. They concluded that the RCSP panels have relatively better capacity to absorb and dissipate energy generated by the dynamic blast load. El-Sisi et al. [12] conducted experimental and numerical study of retrofit systems for RC wall panels for blast mitigation. The results demonstrated that the retrofitted wall panels absorbed significant energy after a support rotation of 10°, which is considered as blowout/ complete collapse by the manual prescribed by USA DoD [41]. Recently, Roy and Matsagar [45] showed that tensile damage induced in the unexposed face of the wall panels under blast loads is comparatively higher than that at the exposed face.

Until date, the analysis and design of structures under such low probability-high consequence (LPHC) blast events have been deterministic in nature. However, in reality, physical properties of structural system, such as dimension of structure, capacity of structural material, etc. as well as the loading phenomena invariably fluctuate, making the current simplified design approaches to be relatively lesser rational. Owing to higher degree of uncertainties in structural parameters and prediction of blast load, obtaining accurate performances of structures under the explosion loads involve extreme difficulties and challenges [24,7]. As a result, the responses tend to show a stochastic nature, which becomes important in determining the reliability aspect of a structural problem, thereby improvising the design guidelines to make robust blast- and explosion-resistant civil structures.

The probabilistic approaches in blast engineering are limited from the viewpoint of investigating performance of RC structural members, especially for RC panel members [32,55,46]. Recently, Olmati et al. [37] and Gombeda et al. [16] developed performance-based frameworks to improve the blast-resistant design of precast concrete wall panels under blast loading scenario. Shi and Stewart [48] conducted reliability analysis to predict risk reduction in RC wall panels subjected to explosive blast loading. They showed that the blast-resistant wall panel has 5% to 100% lower failure probability as compared to a conventional wall panel. Considering other RC structural member, Parisi [40] developed and compared blast fragility of RC columns typically designed in European regions designed under gravity and earthquake load for residential buildings. The proposed framework may be used for quantitative risk analysis and performance-based design of structures under extreme blast loadings. Yu et al. [65] developed an analytical approach to predict the failure probabilities of RC columns under blast loadings. According to them, axial force in columns played a predominant role in affecting the failure probabilities of the RC members. Employing multi-material arbitrary Lagrangian Eulerian (MM-ALE) approach for modeling the blast loading was recommended to study the damage characteristics of RC concrete member under blast loading by Thai and Kim [56]. For RC structural elements under blast loading, the change in failure modes depends on the quantity of energy and energy flow rate imparted to the structural element [57]. Wu et al. [62] recommended that the numerical model established successfully represents the RC slabs structural failure under blast loading. Although few researches are available on stochastic domain to compute the reliability of other RC member, the approaches in assessment were primarily based on single-degree of-freedom (SDOF) simplification. Moreover, material behavior and the subsequent structural response under blast loads possess larger degree of nonlinearity, which involves generation of complex stress states due to stress wave propagation in the structural member, which were primarily neglected in most research documents. In this context, it is imperative to address the challenges concerning structural details and uncertain loadings through proper frameworks, which influences the structural performance comprehensively, as the existing approximate simplified approaches used do not necessarily lead to reliable structural design [30].

Herein, probabilistic assessment of three-dimensional (3-D) RC wall panels is carried out considering material and geometric nonlinearity under surface-burst and free airburst scenarios. High strain rate effect induced in the RC walls due to the blast loads is modeled using available standard dynamic increase factors (DIFs) for concrete and steel. Uncertainty in the system is assumed in material capacity (strength), mechanical loads, and dynamic blast loads considering an appropriate distribution with certain mean and standard deviation. Limit state of failure and the respective threshold limiting values are obtained from the United States Department of Defense (DoD) manual, PDC-TR 06-08. Based on the gaps in literature, the objectives for the current study are: (i) to compare the responses of the wall panels under the surface-burst and free airburst scenarios, (ii) to study the probability of failure for the wall panels by constructing fragility curves, and (ii) to study the effect of uncertainty in input parameters influencing the output response parameters.

2. Structural description and numerical modeling

The three-dimensional (3-D) RC wall panels have planar dimension of 6.1 m × 4.3 m, assuming height of 4.3 m. Different thicknesses of wall panels are considered for the current study in which the RC wall panels are subjected to compressive in-plane axial load at certain eccentricity, representing typical accidental eccentricity in the service loading of RC walls. A single layer of steel reinforcement is embedded in the concrete panels of different thicknesses having clear cover of 25 mm on tension side. Along the longitudinal direction, 12φ rebar spaced at 428 mm center-to-center (c/c) is used as reinforcing elements in the RC wall panels on the tension side, where φ represents diameter of the bar in mm. Similarly, 12φ rebar spaced at 300 mm c/c is used as transverse reinforcements in the RC members, as shown in Fig. 1. The mechanical loads on the RC wall panels are calculated from the dead load (DL) and live load (LL), as per Indian Standard [20]. The mechanical loads along with the accidental eccentricity on the RC panels of different thickness for the RC wall panels are provided in Table 1. Finally, it is assumed that the RC panels are not designed for any blast-resistant material under any accidental blast loads.

2.1. Finite element (FE) modeling and analysis of RC wall panels

The finite element (FE) modeling of RC panels is carried out in a commercial software ABAQUS® [1] to investigate the performance of wall panels exposed to blast considering the effect of material and geometric nonlinearity. Moreover, multiple simulations are carried out through the ABAQUS® scripting interface programmed in object-oriented Python language to incorporate the variabilities in model parameters. The scripting interface is used to access the functionalities of ABAQUS®, and the scripts coded in the interface holds the advantage of performing a number of simulations without intervention of the user.

In the current approach, continuum- and plasticity-based concrete damaged plasticity (CDP) model is used to define the nonlinearity in concrete. The CDP model is capable to capture the degradation of elastic stiffness in both tension and compression state of concrete. The CDP model assumes two key failure mechanisms in concrete: tensile cracking and compressive crushing. The damaged plasticity model considers uniaxial tensile and compressive behavior, which are characterized by respective stresses and cracking/inelastic strains to represent complete inelastic behavior of concrete. The parameters of CDP model are presented in Table 2. The steel reinforcement used to transmit the axial forces is modeled by one-dimensional (1-D) element using the classical metal plasticity

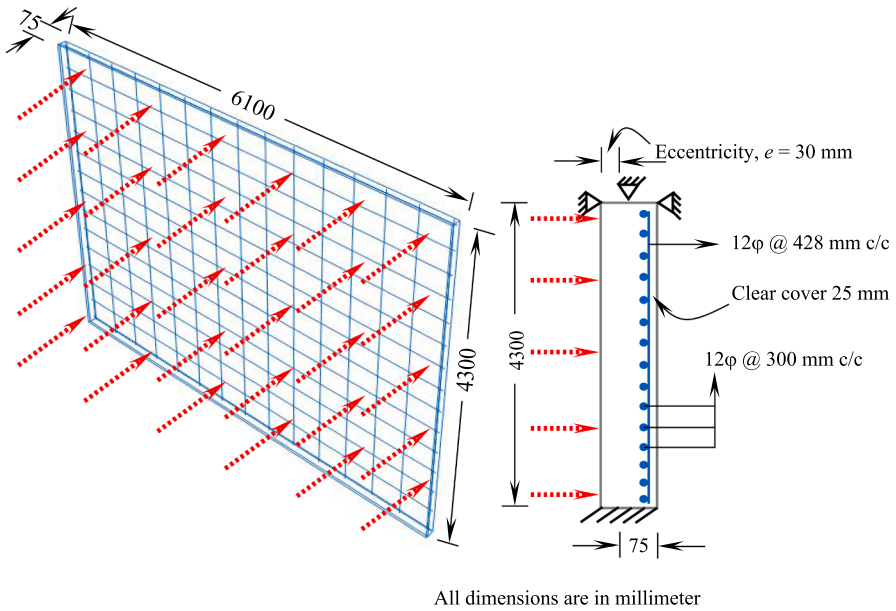

Fig. 1. 3-D view showing blast exposure and sectional cross-section view showing reinforcement details.

Table 1
Accidental eccentricity and mechanical load assumed for the analysis.

Panel member	Member size (mm)	Accidental eccentricity (mm)	Mechanical load (kN/m^2)	
			Dead load	Live load
Compressive in-plane loaded member	75, 100, and 125	30 mm from blast exposure	107.5	320

involving von-Mises yield criterion with associated plastic flow and isotropic hardening. The steel reinforcement bars transmit the axial tensile forces and are modeled using classical metal plasticity law. The plasticity in this model is simulated by providing yield stress for corresponding uniaxial plastic strain. The reinforcing steel is considered to behave as elastoplastic hardening material, i.e., exhibiting bilinear stress–strain law, in both compression and tension, which uses the von-Mises plasticity yield criterion with associated plastic flow and isotropic hardening.

The mesh of concrete geometry is lumped by 8-node trilinear continuum C3D8R element with reduced integration and hourglass control, whereas the mesh of the steel rebar geometry is lumped by 2-node linear truss element T3D2. Embedded constraint available in ABAQUS® solver is used to constrain the translational degrees of freedom of the embedded nodes (steel reinforcement) to transfer the stresses from concrete to steel rebar through the developed nodes. The RC wall members under the compressive in-plane loading is modeled considering fixed boundary condition (BC) at bottom and pinned on other three sides allowing necessary rotations. The boundary conditions in each RC wall panel are given as:

(i) bottom face: DOFs - $u_x\,(1) = u_y\,(2) = u_z\,(3) = \phi_x\,(4) = \phi_y\,(5) = \phi_z\,(6) = 0$, and (ii) remaining sides: DOFs- $u_x\,(1) = u_y\,(2) = u_z\,(3) = 0$.

The BCs assumed for the RC members is shown in Table 3.

The geometric nonlinearity is modeled using NLGEOM option available in ABAQUS® because large displacement is expected, which is directly associated with geometric nonlinearity. The blast loading on the structural panels is applied as pressure loading at the desired surface of exposure, as shown in Fig. 1. Finally, the dynamic explicit analysis is carried out for duration of 5 s and the response at each node is stored for final post-processing.

2.2. Numerical solution approach for blast analysis

Explicit dynamic scheme available in ABAQUS® solver domain is adopted for the analysis of RC wall panels under blast loading. The solver performs dynamic analysis using explicit central difference integration scheme. The solution schemes used to assess the RC wall panels under the dynamic blast loading are discussed hereunder.

The dynamic analysis of RC wall panels under blast loading is performed in explicit domain as it is more efficient for solving wave propagation problems, in which the nonlinear response is obtained incrementally. The discretized equilibrium equation in FE environment is expressed as,

$$\{P\}^{t} - \{I\}^{t} = [M]\{\ddot{u}\}^{t} \tag{1}$$

where, $\{P\}^{t}$ is external force vector, $\{I\}^{t}$ is internal force vector created from element stresses, $[M]$ is diagonal lumped nodal mass matrix, $\{\ddot{u}\}^{t}$ is nodal acceleration at beginning of the increment, and $[M]\{\ddot{u}\}^{t}$ is force vector due to material inertia. Therefore, the nodal acceleration can be obtained as under,

$$\{\ddot{u}\}^{t} = [M]^{-1}\left(\{P\}^{t} - \{I\}^{t}\right) \tag{2}$$

Central difference integration scheme is used to update the velocity and displacement at each node from Eq. (2), which is expressed as,

$$\{\dot{u}\}^{t+\frac{\Delta t}{2}} = \{\dot{u}\}^{t-\frac{\Delta t}{2}} + \left(\frac{\Delta t^{t+\Delta t} + \Delta t^{t}}{2}\right)\{\ddot{u}\}^{t} \tag{3}$$

$$\{u\}^{t+\Delta t} = \{u\}^{t} + \Delta t^{t+\Delta t}\{\dot{u}\}^{t+\frac{\Delta t}{2}} \tag{4}$$

Iterations are not required in equation solver to update the acceleration, velocity, and displacement responses. The analysis using explicit operator is performed using a large number of time-increments of relatively smaller size. However, the central difference integration scheme is conditionally stable and the solution becomes unstable and diverges rapidly if the time increment is too large. In this regard, stability limit for the operator in terms of Eigen value is given by,

Table 2
Parameters used for the concrete damaged plasticity (CDP) model.

Dilation angle (ψ)	Eccentricity (e)	f_{b0}/f_{co}	K_c	Viscosity (μ_e)
36.31	0.1	1.16	0.667	0

Table 3
Boundary condition of the panel members.

Boundary conditions	DOFs
Fixed at bottom and pinned (rotation allowed) on other three sides	Bottom face: u_x (1) = u_y (2) = u_z (3) = ϕ_x (4) = ϕ_y (5) = ϕ_z (6) = 0; All other sides: u_x (1) = u_y (2) = u_z (3) = 0

$$\Delta t \leq \frac{2}{\omega_{max}\left(\sqrt{1+\zeta^2}-\zeta\right)} \tag{5}$$

where, ω_{max} represents maximum Eigen value of the element, and ζ represents fraction of critical damping at highest mode. The stable time increment can be expressed as, $\Delta t \leq \min(L_e/c_d)$, where, L_e is characteristic length of the smallest element in the domain, $c_d = \sqrt{\frac{\widehat{\lambda}+2\widehat{\mu}}{\rho}}$ is dilatational wave speed, where $\widehat{\lambda}$ is first Lamé constant, $\widehat{\mu}$ is shear modulus, and ρ is the density of element, chosen automatically to satisfy the user-defined critical time step. Finally, to minimize numerical errors, it is worthwhile to conduct mesh convergence trials to have insignificant influence on the numerical results without substantially increasing the computation time.

3. Fragility function for probabilistic framework

Fragility estimation has been a common practice in earthquake engineering to determine the probability of failure and investigate the performance of structure against seismic excitations [42,44]. According to performance-based design (PBD) philosophy, structural members are usually designed for a particular level of performance, such as, immediate occupancy (IO), life safety (LS), collapse prevention (CP), or collapse (C) for seismic loadings [13]. Similarly, in blast engineering, the concept of fragility is defined as a probabilistic relationship between failure of a structural member or system (here, RC wall panels) as a function of some measure of extreme loading condition (here, blast loading) for different damage states, which is given as,

$$p_f = P(D \geq C|\mathrm{IM}) \tag{6}$$

where, p_f is the probability that the demand D exceeds the limit state capacity C subjected to blast loading scenario with intensity measure, IM. For the present study, the probability of failure can be expressed as,

$$p_f = P\left(\theta_{dem} \geq \theta_{cap}|w,s\right) \tag{7}$$

where, θ_{dem} represents maximum support rotation for the RC wall panels under a particular level of blast load; θ_{cap} represents resistance of the RC panels in terms of support rotation; and w and s represent the IM parameters adopted here, which are charge weight and standoff distance, respectively. Finally, the fragility curves are constructed using traditional two-parameter lognormal distribution functions, which is given as Shinozuka et al. [49],

$$p_f = \Phi\left[\frac{\ln(x/\mu)}{\sigma}\right] \tag{8}$$

where, x represents the response obtained for the wall panels due to IMs as charge weight or standoff distance.

3.1. Limit state of failure

Performance criteria or limit states of failure are well established for earthquake engineering, which includes definitive criteria such as deflection, inter-storey drift, stresses induced, moment-capacity, etc. However, for antiterrorism design, the response parameters are limited to represent the damage induced in the structure. According to the PDC-TR-06-08 [41], generally two limit states of failure are used as response parameter to provide baseline for minimum protection of structural members, which are support rotation angle (θ) and ductility ratio (μ). These parameters are defined as:

$$\theta = \mathrm{arctg}(2\delta_{max}/L) \tag{9}$$

$$\mu = \delta_{max}/\delta_e \tag{10}$$

where, δ_{max} and δ_e are respectively the maximum and elastic displacement of the structural member. In the current PBD approach, five damage states prescribed in the antiterrorism design guideline, which are superficial damage (B1), moderate damage (B2), heavy damage (B3), hazardous failure (B4), and blowout (B5) are used to compute the failure probabilities of the RC wall panels under surface-burst and free airburst scenarios, as shown in Fig. 2. The threshold values for different damage states are presented in Table 4. On the other hand, examples of potential IMs include explosive mass or charge weight, standoff distance, radial distance, scaled distance, etc. In the present study, charge weight (w) and standoff distance (s) are used as IM parameters for construction of fragility

curves under blast loads. Finally, an algorithm is presented as Fig. 3 to estimate the fragility of RC walls considering the threshold limit states of failure.

3.2. Procedure followed in fragility estimation

Herein, the fragility analysis of RC wall panels is conducted by carrying out a number of simulations in ABAQUS® using Python programming language. In this regard, a nine-step Monte Carlo algorithm is outlined for construction of fragility curves based on the above-mentioned traditional formulation prescribed by Shinozuka et al. [49]. Following this algorithm, Fig. 3 is presented to illustrate the proposed probabilistic framework for obtaining probability of failure for the RC wall panels under blast. The steps involved in generation of the fragility curves are discussed hereunder.

Step 1: Define capacity of RC wall panel, i.e., support rotation capacity (θ_{cap}), corresponding to the threshold limit state.

Step 2: Generate n random independent and identically distributed (iid) samples for each uncertain parameter (here, 6), ξ_i, $i = 1, 2, 3, \ldots, 6$. The random samples for the stochastic parameters are generated based on a certain distribution (mostly, normal and lognormal) considering a mean and CoV.

Step 3: Generate the blast pressure time history curves corresponding to the random samples generated for each level of IM (w and s).

Step 4: Analyze the RC wall panel of a particular thickness for each simulated blast pressure time history curve and subsequently obtain the structural response in terms of support rotation of the structural panel (θ_{dem}).

Step 5: Compare the response support rotation, θ_{dem} with the corresponding rotation capacity, θ_{cap} (Table 4) for the single set of IM parameter. The RC wall panel is considered to fail when the response support rotation exceeds the threshold limit state for each level of IM and for each damage states.

Step 6: Compute the probability of failure (p_f) using Eq. (8) conditioned that the demand (θ_{dem}) reaches or exceeds the capacity (θ_{cap}) for a particular IM level. Similarly, repeat the step for different IM levels and different damage states.

Step 7: Repeat Steps 2 to 6 until the number of simulations (N_f) in which the demand exceeds the capacity is 20.

Step 8: Plot fragility curves with IMs (w and s) for different damage states on the horizontal x-axis and probability of failure on the vertical y-axis.

Step 9: Repeat Steps 2 to 8 to conduct parametric studies for computing the failure probability of the RC wall panels with different thicknesses, independently.

4. Uncertainties associated in the probabilistic framework

The concept of fragility in blast engineering requires proper understanding of variabilities and uncertainties associated in the system. In presence of these uncertainties, estimating accurate level of reliability for structures should be the primary aim as the existing blast-resistant design guidelines are based on deterministic codes. To begin with, the intensity of blast loading is considered as the primary source of uncertainty, which includes distribution, nature, and quantity of explosive materials in the compartment or any open space, distance of explosion from the target structure, etc. Moreover, member size, nature of induced mechanical load, and strain-rate dependent nonlinear mechanical properties of material also tend to influence the structural responses, which also possess a fair degree of uncertainty. Therefore, such risk assessment strategy should include uncertainty in whole system to achieve safety of structures under extreme blast scenario.

4.1. Uncertainty in mechanical properties

Uncertainties associated with material models have the potential to impact the resultant structural reliability under blast loading.

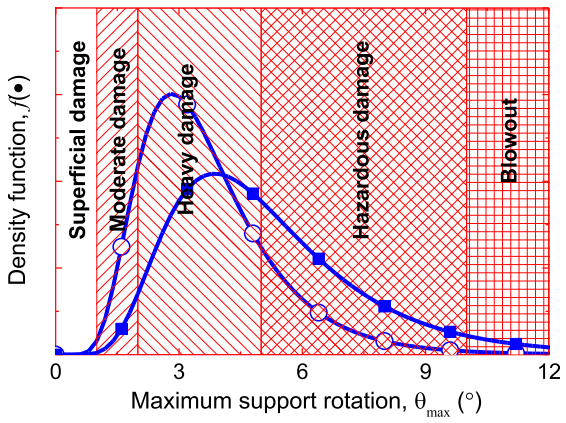

Fig. 2. Damage criterion considered for the RC wall panels.

Table 4
Threshold values for considered damage levels [37].

Damage level	Support rotation, θ_{max} (°)	Ductility, μ
Superficial damage (B1)	≤1	<1
Moderate damage (B2)	≤2	–
Heavy damage (B3)	≤5	–
Hazardous failure (B4)	≤10	–
Blowout (B5)	>10	–

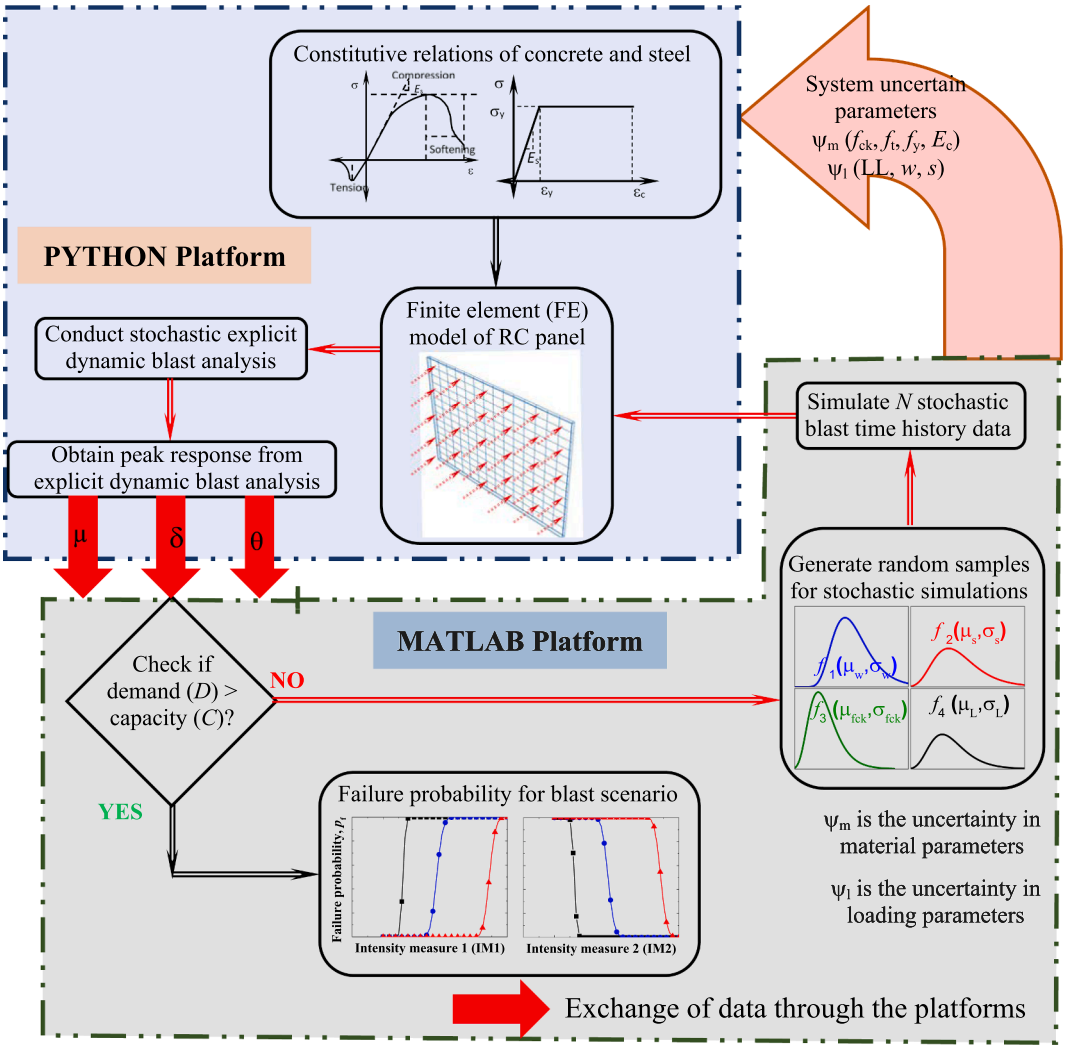

Fig. 3. Framework for fragility estimation of the RC wall panel under blast.

The mechanical properties determining the performance of RC structure exposed to blast is compressive and tensile strength, modulus of elasticity, and the subsequent stress–strain response. Due to inherent uncertainties in mechanical properties, the actual resistance of RC members differs from their nominal capacity. In this context, the compressive strength is chosen as the parameter influencing the performance of RC members. Using the compressive strength, the stress–strain relationship of concrete under dynamic condition is obtained from the formulations provided in CEB-FIP Model Code 1990 (1993). Several research works have been carried out to investigate the effect of uncertainty in the mechanical strength of the material [6,66]. Most of the studies conducted until date have assumed variability of about 10% to 15% in the mechanical strength of the materials assuming lognormal distribution as best fit to obtain realistic response. Hence, in the present study, the uncertainty in strength of concrete and steel is assumed as 10% with lognormal distribution as appropriate fit.

Furthermore, in order to simulate the real behavior of the RC wall panels under the effect of these loadings (blast loads under

constant gravity loads), strain-rate dependent properties need to be defined explicitly. The blast loading causes a relatively higher strain rate of about 10^2 s^{-1} to 10^4 s^{-1} on the structure [33], and the behavior of RC material under such strain-rate effect is relatively different as compared to the behavior under lower static or quasi-static strain-rate effect. The dynamic behavior of concrete materials is more complex primarily due to brittle natured- and hydrostatic stress dependent properties. Further, under the dynamic conditions, the stress–strain responses are affected by several other factors, which include the Stefan effect (presence of free water), radial or lateral and axial inertia, etc.[4]. Therefore, the dynamic attributes of concrete are presented in terms of dynamic increase factors (DIFs) that relates to the degree of dynamic stress in comparison to the static/ quasi static stress. In this regard, models proposed by Al-Salloum et al. [4] and Zhou and Hao [67] are used to calculate the dynamic increase factors (DIFs) for a set of strain rates respectively under compression and tension. Subsequently the dynamic compressive and tensile strengths of concrete are computed by multiplying the respective DIFs with the strengths in static/ quasi-static conditions.

On the other hand, under high strain-rate effect, the yield and ultimate stresses of reinforcing bars generally increase depending on the grade of steel used. The main source influencing the strain-rate effect is the yield strength of the steel, which remains as the main source of scatter. In addition, the yield strength is more strain-rate sensitive than the ultimate strength. However, as the yield strength increases, the effect of the strain-rate is relatively less significant [53]. Considering these criteria, the constitutive relation of the reinforcing steel under quasi-static state is adopted from the literature published by Silva and Lu [51]. Thereafter, the dynamic strengths of steel rebar are calculated by using the DIFs obtained from Asprone et al. [5]. The uncertainty is assumed in the characteristic yield strength of steel, which in turn affects the dynamic strength achieved due to higher strain rate. In this study, a coefficient of variation (CoV) of 10% is assumed for the characteristic strength of steel fitted with lognormal distribution.

4.2. Uncertainty in mechanical load

Uncertainties are mostly inherent in case of mechanical (dead and live) loads for existing real structures, and due to these intrinsic variabilities, significant challenges are faced in investigating the structural safety using deterministic analysis. Hence, the variability in mechanical loads is generally considered through classical probabilistic representation. Typically, dead loads do not vary generally throughout the design life of structure. However, few studies have recommended a CoV of 10% assuming the dead load follow normal distribution [11,36]. Similarly, live loads are also characteristically uncertain, which conversely depend on the floor area under consideration. For design purpose, combination of sustained and transient live loads is necessary to consider, which is expected to occur during the design life of the structure. Studies show that the combined maximum live load is modeled using Extreme Type-I distribution with CoV of 25% [10,11]. Therefore, the present study is carried out considering 10% CoV with normal distribution for the dead load and 25% CoV with Extreme Type-I for the live load.

4.3. Uncertainty in blast load

Design blast loads are generally expressed in terms of peak overpressure generated after multiple reflections from adjacent structures. The attained reflected peak overpressure heavily depends on a number of variables, such as, weight of explosive mass, standoff distance, scaled distance, etc. which have great deal of uncertainty in their values. For instance, tolerance or CoV for military blocks of weight 32.6 lb is 0.063 lb which is equal to 0.19%, assuming a lognormal distribution [54]. Simple or non-commercial explosives, such as ammonium nitrate fuel oil (ANFO) may exhibit relatively higher variabilities, up to 50% assuming lognormal distribution [54]. The variability of the system also depends on the range, i.e., standoff distance, which indicates placement of the explosives and the type of guidance system used. The CoV for stand-off ranges differently for different instances, such as, CoV = 0 for explosive ordnance storage, suicide bomber, etc., CoV = 10%−25% for a terrorist vehicle-borne improvised explosive device (VBIED), and CoV up to 30% for collateral damage estimation (CDE) from military weapons [35]. Therefore, in the current study, variabilities in the blast loading is considered through a mean blast load of equivalent trinitrotoluene (TNT) with CoV of 10% having lognormal distribution. Several relationships are available until the date to compute the amplified peak reflected blast pressure and the corresponding blast pressure history [14]. For the present study, empirical relationships provided by Kinney and Graham [25] are used, which involves incident pressure (P_{pos}) and positive phase duration (t_{pos}) to compute blast overpressure history. Finally, the peak reflected pressure, $P_r = C_r P_{pos}$ is computed using the coefficient of reflection (C_r) charts provided in the Unified Facilities Criteria, (UFC) 3-340-02 [58].

5. Sensitivity analysis

Sensitivity analysis indicates how different sources of uncertainty in model input is apportioned to the model output [47]. In other words, the most contributing input variables influencing the output behavior of model is determined [28]. The contribution of input variables in the system may be individual (first order) or the input variables may have some interaction effects (second or higher order) in the system. In the present study, MC-based Sobol sensitivity indices are estimated by decomposing the output variance into contributions associated with each input factor [52,29]. Let us assume for any arbitrary model, the output Y depends on several input independent random variables, X_1, X_2, …, X_p, which is given as,

$$Y = f(X_1, X_2, \cdots, X_p) \tag{11}$$

Decomposing Eq. (11) in terms of increasing dimensionality,

$$f(X_1, X_2, \cdots, X_p) = f_0 + \sum_{i=1}^{p} f_i(X_i) + \sum_{1\le i<j\le p} f_{ij}(X_i, X_j) + \cdots + f_{1,2,\cdots,p}(X_1, \cdots, X_p) \tag{12}$$

Moreover, depending on the mutual dependence of the input variables, a unique decomposition exists such that all the summands are mutually orthogonal. Using this assumption, the variance of the output, $V(Y)$ can also be decomposed into,

$$V(Y) = \sum_{i=1}^{p} V_i + \sum_{1\le i<j\le p} V_{ij} + \cdots + V_{1,2,\cdots,p} \tag{13}$$

where, V_i, V_{ij}, $V_{1,2,\ldots,p}$ denote the variance of f_i, f_{ij}, $f_{1,2,\ldots,p}$, respectively, which are given as,

$$V_i = V(E(Y|X_i)) \tag{14}$$

$$V_{ij} = V(E(Y|X_i, X_j)) - V_i - V_j \tag{15}$$

$$V_{1,2\cdots,p} = V(Y) - \sum_{i=1}^{p} V_i - \sum_{1\le i<j\le p} V_{ij} - \cdots - \sum_{1\le i_1<\cdots<i_{p-1}\le p} V_{i_1,\cdots,i_{p-1}} \tag{16}$$

From this decomposition, the sensitivity indices are obtained, which are given as,

$$S_i = \frac{V_i}{V(Y)} = \frac{V(E(Y|X_i))}{V(Y)} \tag{17}$$

$$S_{ij} = \frac{V_{ij}}{V(Y)} = \frac{V(E(Y|X_i, X_j)) - V_i - V_j}{V(Y)} \tag{18}$$

$$S_{1,2,\cdots,p} = \frac{V_{1,2\cdots,p}}{V(Y)} = \frac{V(Y) - \sum_{i=1}^{p} V_i - \sum_{1\le i<j\le p} V_{ij} - \cdots - \sum_{1\le i_1<\cdots<i_{p-1}\le p} V_{i_1,\cdots,i_{p-1}}}{V(Y)} \tag{19}$$

Expressions in Eqn 17, 18 and 19 are termed as first-, second-, and p^{th}-order sensitivity indices. It can be noted that the second- and higher-order sensitivity indices have interactions of the factors, X_i, X_j, …, X_p.

In the present study, first-order sensitivity index is computed to obtain the influence of the input variables on the output response. Here, the influences of five input variables are examined, which includes charge weight, standoff distance, strength of concrete and steel, and axial live load in terms of eccentric loading on the wall panel. It has been found that the dead load acting along the plane of the wall panel has no considerable contribution to the blast response of the panels, in currently considered simulations, since no additional moment is induced in the walls to alter the blast responses. Finally, the output response is obtained in terms of maximum rotation and stress induced in the wall panel.

6. Numerical study

Herein, three-dimensional (3-D) RC wall panels of different thicknesses are studied exposed to surface-burst and free airburst loadings considering nonlinearity in material and geometric properties. The RC panels have planar dimension of 6.1 m × 4.3 m with thicknesses varying as 75 mm, 100 mm, and 125 mm. Due validation has been conducted using the results reported by Jain et al. [22], which is presented hereunder.

A three-dimensional (3-D) FE model is developed for a square RC wall having dimensions 2 m × 2 m with thickness of 200 mm, as analyzed by Jain et al. [22]. The FE model is developed using 3-D part option in ABAQUS®, in which a single layer or single mat of two-way steel reinforcement, perpendicular to each other is provided in which a concrete clear cover of 75 mm according to IS 456 [19] is maintained. The layers of reinforcements are created as separate part and assembled using embedded option to assume full bonding and further transfer the stresses from concrete to steel. The CDP model is used to simulate stress–strain behavior in concrete for both strain rate dependent and rate dependent stimulations. The steel reinforcement is modeled using the plasticity model for strain rate dependent simulations. The RC panel is modeled using 3-D continuum 8-node linear brick element (C3D8R) with reduced integration and hourglass control. The steel rebar is modeled using 2-node linear 3-D truss (T3D2) element. All four sides of the concrete walls are restrained in three Cartesian directions, i.e., x, y, and z. The interaction between concrete and the rebar is modeled with the embedded region option available in the ABAQUS®. Blast load is simulated as an equivalent triangular pressure pulse calculated using UFC 3-340-02 [58]. The analyses are performed for a peak blast overpressure of 1.162 MPa, with wave arrival time as 1.59 ms, and positive phase duration as 6.14 ms. The study is conducted for total step time of 7 ms, and the results are compared with the study published by Jain et al. [22]. The concrete grade for the current study is taken as M25. The Young's modulus (E), Poisson's ratio (μ), and mass density (ρ) assumed for concrete are taken from the published work. The tensile strength of concrete is calculated as $0.7\sqrt{f_{ck}}$. The steel reinforcement used is Fe415 grade steel with static tensile yield stress, $\sigma_t = 415$ MPa. The model is validated, and the results obtained in the present study are compared with the published results. The comparison of the results is shown in Fig. 4. The accuracy of the results for the displacement response is observed to be in range of 95% to 98%, whereas the peak principal stress obtained through the present numerical strategy has good match with that of the existing study, which shows the validation of the proposed modeling strategy.

Mesh convergence trials are conducted to determine optimum mesh size to produce significant results. The mesh size for concrete, thus obtained for the current analysis is 60 mm × 60 mm × 60 mm. For surface-burst scenario, the reflected blast wave is simulated by multiplying the charge weight by 1.8 because it is assumed that the reflected pressure increases many-folds upon encountering a rigid surface before incident on the target structure [24]. On the other hand, under free airburst scenario, the generated reflected blast pressure propagates spherically in outward direction and causes impact on the structure without encountering any reflections. The 3-D RC wall panels are analyzed considering single side exposure of blast loading, which is to the opposite face of the tension reinforcement. The blast responses of the RC wall panels are studied in terms of deflection, rotation, induced stress, and plastic strain at the center of the RC wall panels. The uncertainties in the system are assumed in material strength of concrete and steel, axial live load in terms of eccentricity in wall loading, intensity of blast load in terms of charge weight and standoff distance. Relevant distributions, considering the respective deterministic values, are assumed to conduct the probabilistic study, which are provided in Table 5, and the corresponding distributions are presented in Fig. 5. Moreover, probability density function (PDF) curves are obtained to observe the nature of responses obtained from the blast analysis. Finally, the cumulative distribution function (CDF) curves are constructed to investigate the vulnerability of the RC panels under the surface-burst and free airburst loadings.

6.1. Results and discussions

Fig. 6 illustrates out-of-plane deflection (δ_b) and principal stress ($\sigma_{11,b}$) at the unexposed side of wall panels for different thicknesses under surface-burst and free airburst loadings. The deflections of wall panels under the surface-burst scenario are substantially higher as compared to free airburst scenario. This is primarily due to the effect of multiple reflections along the propagation, which significantly alters the loading intensity. The peak deflections observed are 538.17 mm, 305.65 mm, and 178.22 mm, respectively for the panels with thicknesses from 75 mm to 125 mm under the surface-burst scenario. On the other hand, under the free airburst scenario, the peak deflections respectively observed are 198.26 mm, 102.27 mm, and 51.24 mm. Therefore, due to the nature of blast, the peak responses have increased by ~2.7 to 3.5 times for the surface-burst scenario as compared to free airburst scenario.

Moreover, residual deflections for the wall panels are also investigated under the blast scenarios. The residual deflections for the panels are observed to be 505.45 mm, 223.18 mm, and 108.15 mm, respectively for increasing panel thicknesses under the surface-burst scenario. In contrary, under the free airburst scenario, the residual deflections observed are 113.58 mm, 42.27 mm, and 11.25 mm, respectively. The residual response is also an indicator of the degree of damage induced in the structural member. The residual responses have increased by ~4.4 to 9.7 times for the surface-burst scenario as compared to free airburst scenario. This indicates that the panels under surface-burst scenario have induced ~4.4 to ~9.7 times the damage as compared to the free airburst scenario. Although the coefficient of reflection for the surface-burst scenario used is 1.8, the response of the panels increases by ~2.7 to 3.5 times, and the residual deflections increase by ~4.4 to ~9.7 times, which show the extent of damage induced in the RC panels. The influence of the coefficient of reflection is thus notable which induces increase of ~1.5 to 2.0 times in the peak displacement response and increase of ~2.5 to 5.4 times in the residual deflection. Furthermore, stress ($\sigma_{11,b}$) history at the unexposed side of the wall panels is also plotted. The stresses developed in the 75 mm thick wall panel is significantly more as compared to the panels of other thicknesses under both surface-burst and free airburst scenarios. On a similar note, the stresses increase from ~1.5 to 2.2 times for the wall panels with thicknesses increasing from 75 mm to 125 mm exposed to both surface-burst and free airburst scenarios. Hence, based on the numbers depicted above, it is necessary to address the type of blast loading in design and protection of structural members against such extreme loading scenarios.

Fig. 7 indicates a set of box plots obtained for maximum rotation (θ_b), strain ($\varepsilon_{11,b}$), and principal stress ($\sigma_{11,b}$) responses for the wall panels with different thicknesses. It is observed that the rotation and strain responses have relatively more skewness as compared to the

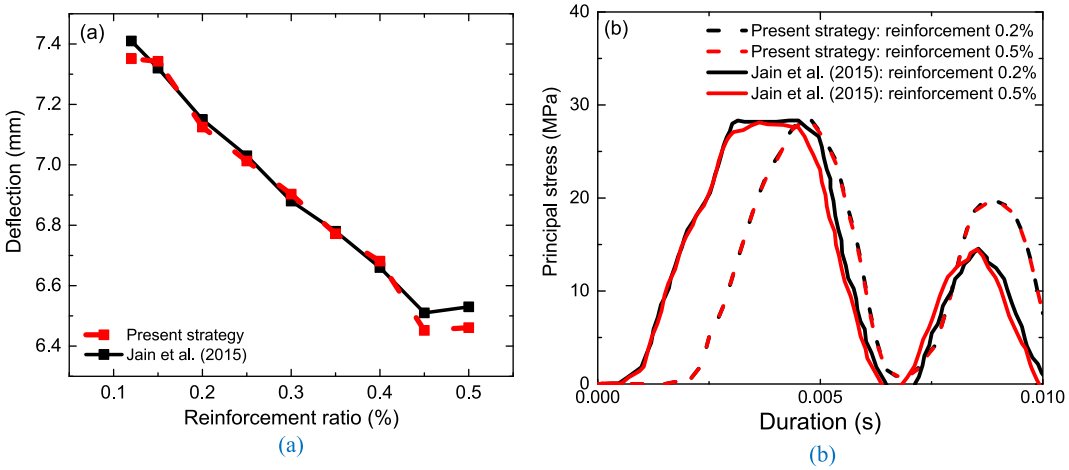

Fig. 4. (a). Comparison of maximum central deflection using present modeling strategy and Jain et al. [22]. Fig. 4(b). Comparison of principal stress using present modeling strategy and Jain et al. [22].

Table 5
Deterministic and stochastic parameters used for the thermo-mechanical analysis.

	Parameters	Unit	Distribution	Mean values	COV
Material properties	Strength of concrete (f_{ck})	MPa	Lognormal (Van Coile et al., 2013)	30	0.1
	Strength of steel (f_y)	MPa		415	
Geometric properties	Size of panels	m^3	Deterministic	Fig. 1, and Fig. 2	–
	Reinforcement details	mm^2			
Mechanical loading	Wall Dead load	kN/m^2	Normal[36]	Table 1	0.1
	Live load		Extreme Type – I [11]		0.25
Blast loading	Charge weight (w)	kg	Lognormal	200	0.1
	Standoff distance (s)	m	Lognormal	15	0.1

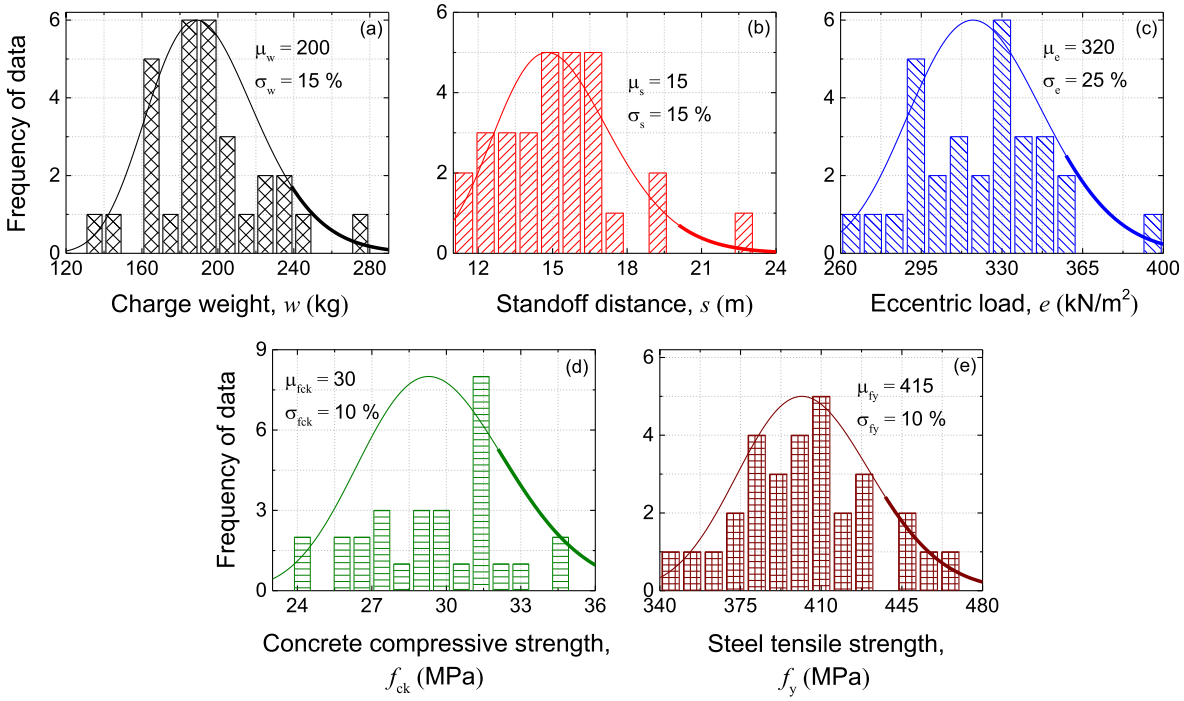

Fig. 5. PDFs and corresponding histograms of the input parameters.

stress response under the surface-burst scenario. On the other hand, under the free airburst phenomena, all responses for the 75 mm and 100 mm thick panels are relatively skewed as compared to the 125 mm thick wall panel. Moreover, the degree of skewness may also be observed from the difference of mean and median lines in the plots. Another interesting observation is that the responses for the 75 mm thick panel for both surface-burst and free airburst scenarios are significantly higher as compared to the other panels. The responses for the other 100 mm and 125 mm thicker panels are comparable, which indicates on increasing the panel size from 100 mm to 125 mm, there is no substantial increase in the responses. Hence, depending on the exposure type, it is recommended to use wall panels of sizes more than 100 mm.

Fig. 8 illustrates the distribution adopted to study the nature of the responses for the wall panels. Mostly, the responses follow lognormal distribution, and the subsequent calculations performed and plots obtained are based on lognormal distribution of the response data. Fig. 9 shows the density function curves for maximum support rotation of the wall panels under the desired blast exposures. The mean support rotations for the wall panels with increasing thicknesses are 8.15°, 4.72°, and 2.82°, respectively. On comparing with the maximum deterministic response, the values obtained are 9.94°, 5.77°, and 3.31°, respectively, which demonstrates that there is a difference from ~17% to 22%. Therefore, there is a significant difference observed for the values, which indicate the effect of uncertainty predominant in this scenario. Further, the support rotations of wall panels under the free airburst scenario are also compared, and in contrary, the mean response is observed to be relatively close with the deterministic response. However, the % difference in the mean and deterministic values is up to 10%, which also indicates a fair influence of stochasticity in the system. Moreover, the coefficient of variation (CoV) for the density curves also indicates the degree of randomness obtained for the responses, although the input parameters mostly have CoV of 10%. Therefore, the degree of uncertainty, i.e., material and loading uncertainty induced in the system has significant influence in the response of wall panels under the considered blast loading scenarios. In this regard, it is recommended to use more rational stochastic approach in developing new guidelines for designing new and retrofit

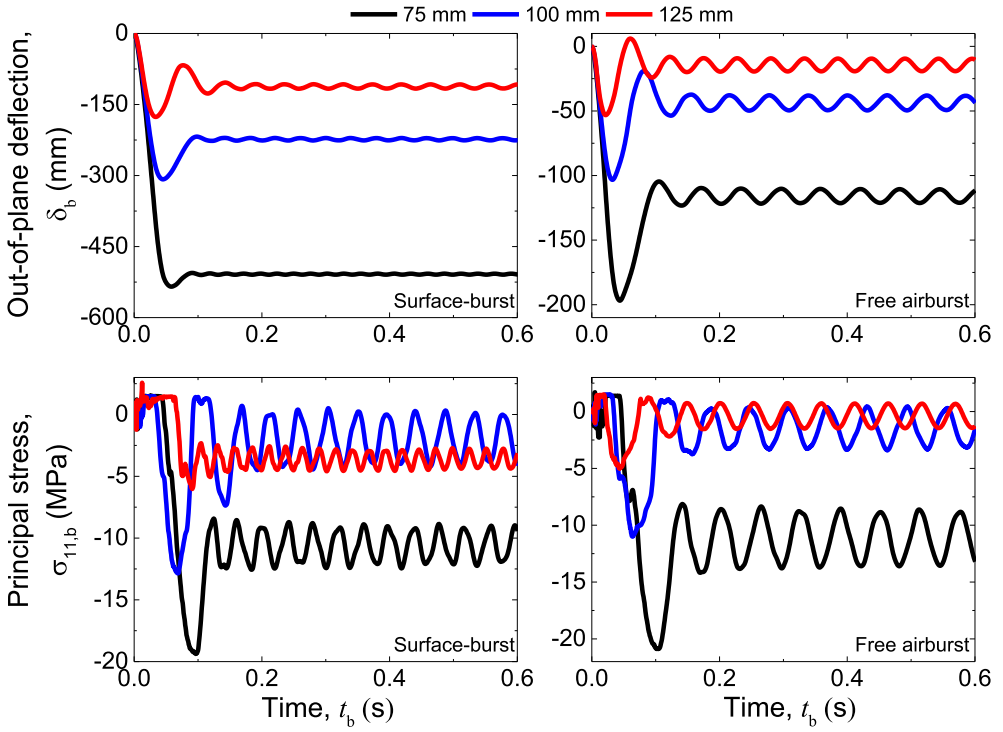

Fig. 6. Out-of-plane displacement and principal stress of the RC wall panels under surface-burst and free airburst scenarios.

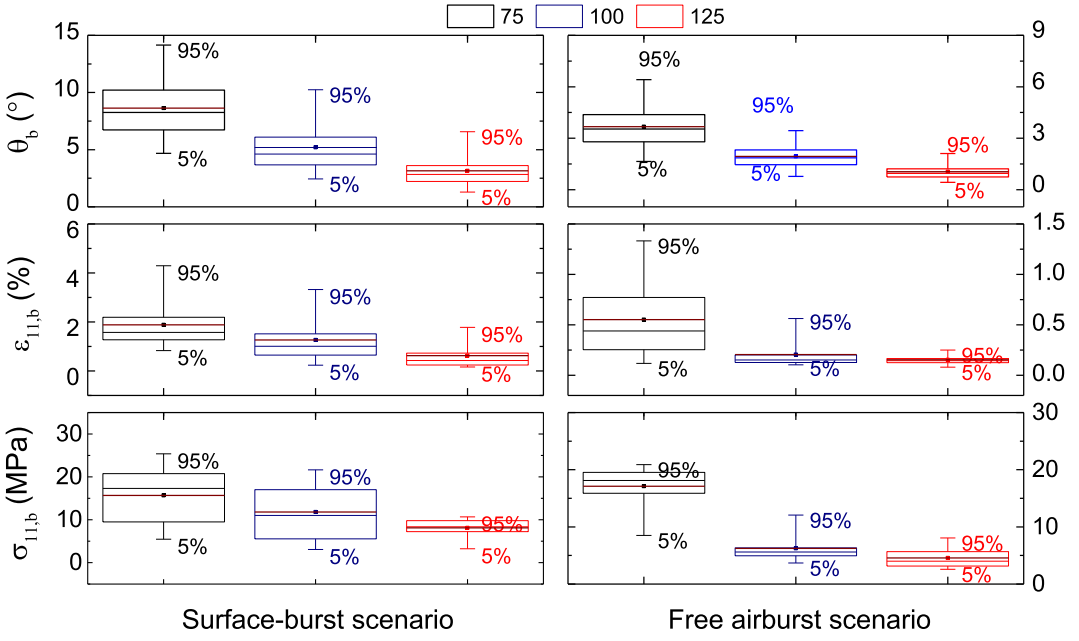

Fig. 7. Box plots representing the degree of uncertainty in the obtained blast responses of the RC wall panels.

existing structures under the effect of scenario-based blast loads.

Fig. 10 shows the degree and nature of damage induced in the wall panels obtained from the threshold values of limit state of support rotation. For the 75 mm thick wall panel under the surface-burst scenario, almost all the responses fall under moderate (B2) and heavy damage (B3) category, more than 75% of the response show hazardous damage (B4), and more than 20% demonstrate blowout (B5) damage. Under the free airburst scenario, few responses suffer no damage or superficial damage (B1), almost all responses show moderate damage (B2), more than 80% responses show heavy damage (B3), more than 30% responses show hazardous

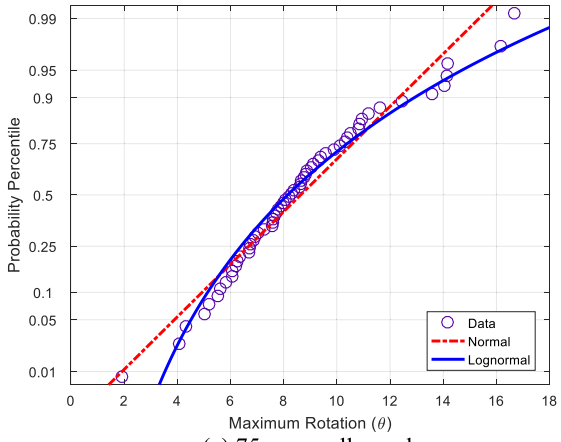

(a) 75 mm wall panel

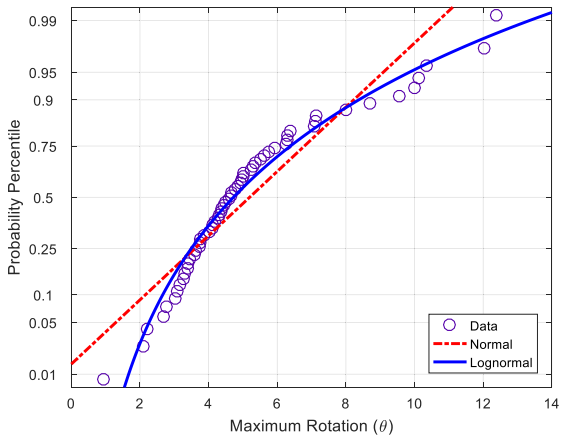

(b) 100 mm wall panel

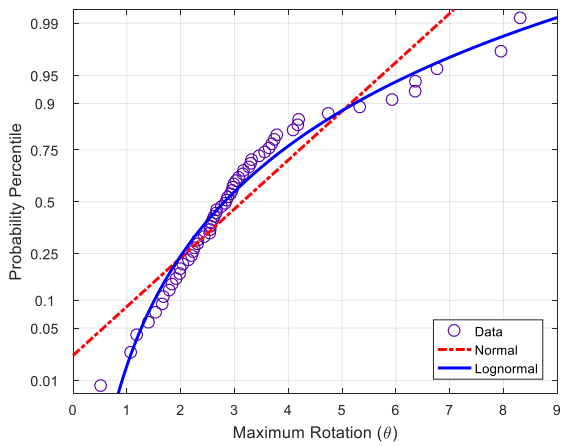

(c) 125 mm wall panel

Fig. 8. Data observation for normal and lognormal distribution under surface-burst scenario.

failure (B4), and no response is observed to demonstrate blowout (B5). Similar observation is carried out for the 100 mm and 125 mm thicker wall panels. Moreover, the mean and deterministic responses are compared to observe the degree and nature of damage inflicted in the wall panels. The mean responses for the 75 mm thick panel show that the wall panel under the surface-burst and free airburst scenarios is inflicted with hazardous failure (B4) and heavy damage (B3), respectively. The deterministic responses are also compared and is observed to have the same B4 and B3 damages, respectively under the surface-burst and free airburst scenarios. It is interesting to note that the mean response for the 100 mm thick panel is observed to have heavy damage (B3); whereas, the deterministic response is observed to have hazardous failure (B4) under the surface-burst scenario. Similarly, the mean response for the 125

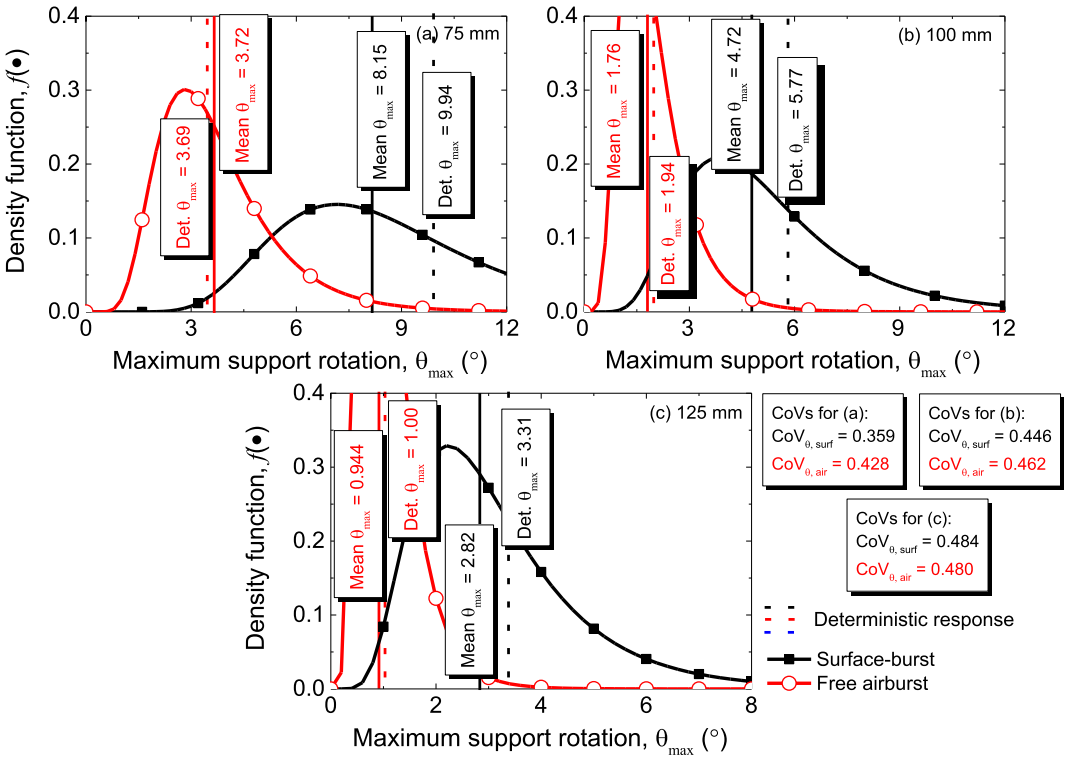

Fig. 9. PDF of the support rotation for the RC wall panels under the surface-burst and free airburst scenarios.

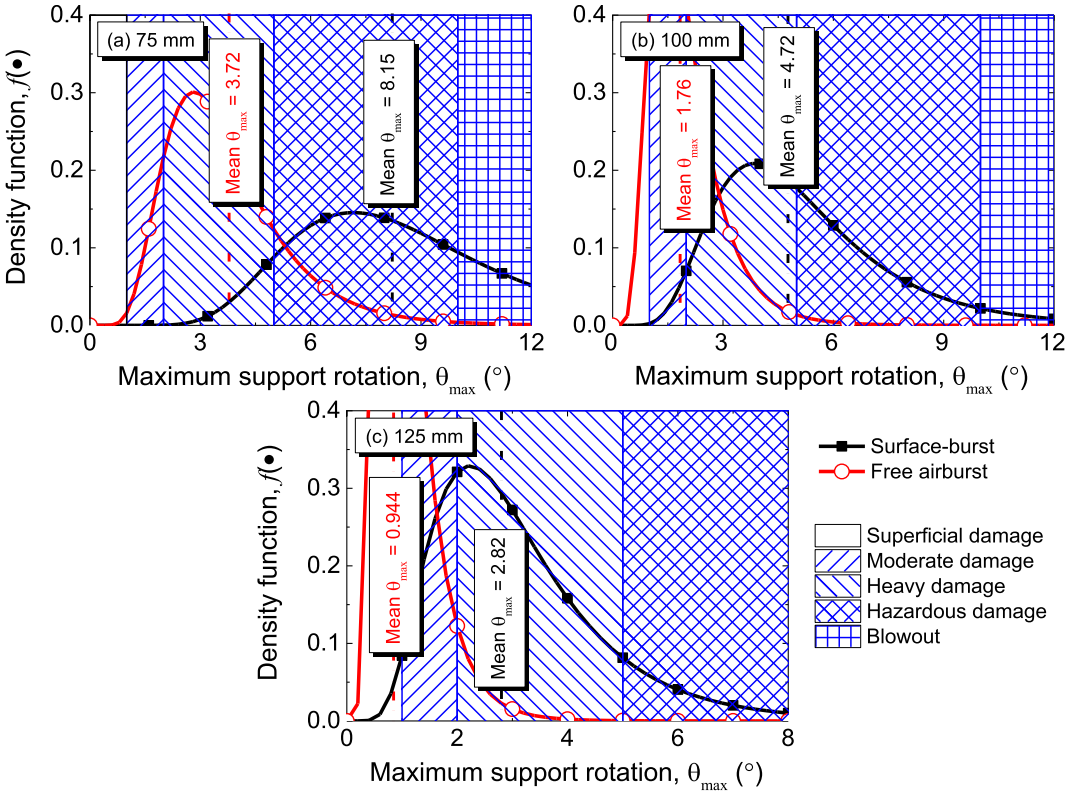

Fig. 10. Observation of different levels of damage for the RC wall panels under surface-burst and free airburst scenarios.

mm thick panel is observed to have superficial damage (B1); whereas, the deterministic response shows the wall panel is inflicted with moderate damage (B2) under the same surface-burst scenario. Therefore, the prescriptive design approach utilizing the deterministic approach may overestimate the design values, which may not essentially evaluate the structural response accurately.

Figs. 11–14 show the fragility curves for the RC wall panels under the surface-burst and free airburst scenarios for IM parameters as standoff distance and charge weight, respectively. The fragility curves under the two types of blast scenario demonstrate that the steepness of the curves for the standoff distance parameter is relatively higher as compared to the fragility curves for the charge weight parameter. This indicates that with slight increase in the IM parameter, the probability of failure increases relatively more for the curves considering standoff distance. From Fig. 11, it is inferred that the probabilities of failure decrease on increasing the wall thickness for all damage types. It is interesting to note that the failure probability of heavy damage (B3) in 125 mm thick panel is relatively higher for standoff distance of more than 17.5 m as compared to the 100 mm thick panel. For distance less than 17.5 m, the failure probability of B3 damage for the 100 mm wall panel increases significantly as compared to the 125 mm thick wall panel. For the deterministic scenario, the failure probability for the 75 mm thick wall induced with moderate damage (B2) to blowout (B5) are respectively obtained as 1, 1, 1, and 0.094, which indicates that considering the uncertainties induced in the system, the failure probability for the blowout (B5) is significantly small. Similarly, for the 100 mm and 125 mm thick panels, the probabilities of failure considering different damages are 1, 1, 0.122, and 0, and 0.904, 0.711, 0.051, 0, respectively. This shows that for a particular standoff distance, with increase in wall thickness from 100 mm to 125 mm, the probabilities of failure decrease by ~10% for moderate damage (B2), ~ 30% for heavy damage (B3), ~ 95% for hazardous failure (B4), and 100% for blowout (B5). Therefore, based on the expected intensity of blast and performance level required by the user, the thickness of the wall panels may be assumed accordingly.

Fig. 12 shows the probability of failure curves for the RC wall panels with charge weight as IM parameter under the surface-burst scenario. It is also interesting to note that the damage states from moderate (B2) to hazardous failure (B4) are significantly high for all the wall panels as compared to the blowout (B5). For 75 mm thick panel, the failure probability for moderate damage (B2) initiates from a significantly lower charge weight (~25 kg); whereas, for the blowout (B5), expected charge weight to initiate the failure is ~100 kg. On the other hand, for the 100 mm and 125 mm thicker panel, the failure probability initiates from ~33 kg and 50 kg for moderate damage (B2); whereas, for the blowout (B5), anticipated charge weight to initiate the failure is ~130 kg and 200 kg. In this context, with increase in thickness of wall panel from 100 mm to 125 mm, the initiation of failure probability requires a significant increase in charge weight by more than 50% for any level of damage.

Fig. 13 illustrates the probability of failure curves for the RC wall panels of different thicknesses under free airburst scenario. On close observation of the failure probability curves, the curves for the 125 mm thicker wall have relatively more shift to the left side as compared to the lesser thick walls. This indicates that the failure decreases at a relatively lower standoff distance for the 125 mm thick panel as compared to the other wall panels, which have comparable failure probabilities at a particular standoff distance. Considering deterministic scenario, the failure probabilities for the 75 mm thick wall panel for moderate damage (B2) to blowout (B5) are obtained as 1, 0.971, 0.085, and 0. Similarly, for the 100 mm thick panel, the failure probabilities obtained respectively are 1, 0.889, 0, and 0. However, no failure is obtained for the 125 mm thick wall panel for the deterministic scenario. Upon comparing the failure probabilities with the surface-burst scenario for the considered damage states, it is observed that there is no/ lesser decrease (~3% to 11%) in the failure probability of the 75 mm and 100 mm thicker panels for the moderate (B2) and heavy (B3) damages, respectively. However, there is significant decrease (91.5% to 100%) in failure probability under free airburst for the 75 mm and 100 mm panels induced with hazardous failure (B4); whereas, there is 100% decrease for all damage states in the 125 mm thick panel. Hence, it can be concluded that the 125 mm thick RC wall panel may be used for such anticipated level of blast as the safety level in terms of failure probability are relatively higher.

Fig. 14 represents the fragility curves for the RC wall panels under free airburst scenario for charge weight IM parameter. The failure curves for the 125 mm thick wall panel demonstrate that the failure probabilities are significantly less as compared to the other less thicker walls. On similar observation carried out for the surface-burst scenario, the damages from moderate (B2) to blowout (B5) for the 75 mm thick panel initiates from a lower charge weight of ~25 kg to a significant weight of ~210 kg, respectively. Moreover, for the 100 mm and 125 mm thicker panels, the damage states trigger from ~70 kg to ~300 kg and ~100 kg to ~310 kg, respectively. Further, on comparing with the charge weights required to trigger the damage states under surface-burst scenario, it is observed that an increase of charge weight by 110% is required to initiate blowout (B5) damage for the 75 mm thick panel. Moreover, an increase of charge weight from ~110% to ~130% is required to initiate moderate damage (B2) to blowout (B5) for the 100 mm thick panel, and from ~55% to ~100% for the 125 mm thick panel. Although, the increase is relatively less for the 125 mm thick wall panel, the charge weight required to initiate failure for the 125 mm panel is significantly more, which allows to take a rational decision that 125 mm thicker RC wall panel may be used in practice in regions, such as, urban and suburban areas, where such intensity of blast loading is expected.

Furthermore, Table 6 is presented to show the difference in charge weight required to cause 50% failure probability for all damage states induced in the wall panels under surface-burst and free airburst scenarios. The consideration of 50% failure probability is not presented in any guidelines or research documents for safety and survivability, however, was selected only to compare the effect of blast exposures in a quantitative manner. For the given wall panels, the increase in charge weights to induce 50% failure probability for moderate damage (B2) are 27.77%, 110.27%, and 94.93%, respectively. This indicates that for the 75 mm wall panel to have moderate damage (B2) with 50% failure probability, the increase in charge weight for free airburst required is relatively smaller; whereas, the increase is significantly higher for the thicker 100 mm and 125 mm wall panels. Similarly, an increase in weight by ~65% to ~93% and ~57% to ~86% for free airburst is required to induce 50% failure probability for heavy damage (B3) and hazardous failure (B4). Hence, it becomes important to consider the type of blast exposure in order to have a rational design for protection of structures against accidental blast loads.

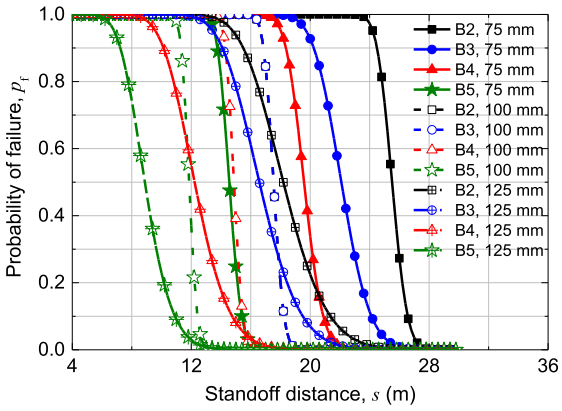

Fig. 11. Fragility curves of the RC wall panels members under surface-burst scenario considering standoff distance as intensity measure parameter.

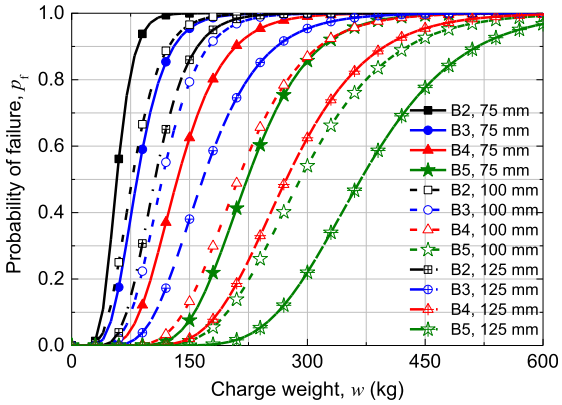

Fig. 12. Fragility curves of the RC wall panels members under surface-burst scenario considering charge weight as intensity measure parameter.

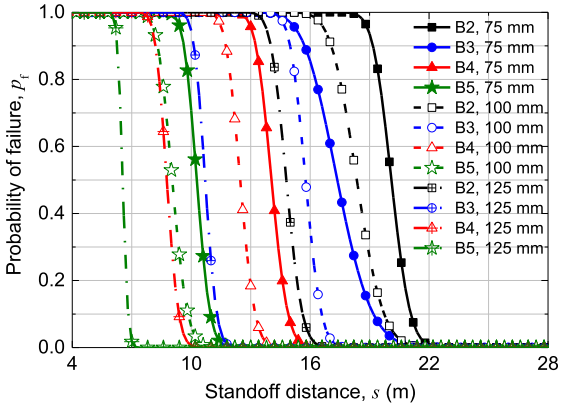

Fig. 13. Fragility curves of the RC wall panels members under free airburst scenario considering standoff distance as intensity measure parameter.

Finally, Fig. 15 is presented to show the first-order Sobol sensitivity indices to demonstrate the influence of input variability on the output responses for the 125 mm RC wall panel under surface-burst and free airburst loads. The indices also indicate the most important parameters influencing the blast response of structures. The sensitivity indices are studied for maximum wall rotation and principal stress as these responses mainly govern the antiterrorism design of structures subjected to explosive blast loads. Under the surface-burst scenario, the maximum rotation is entirely influenced by the charge weight (~65%) and standoff distance (~31%), which in turn relates to the intensity of blast loading. Similarly, under free airburst scenario, the charge weight (~84%) and standoff distance (~15%) mostly influences the degree of change in rotation of the RC wall panels. For either blast load scenarios, these two

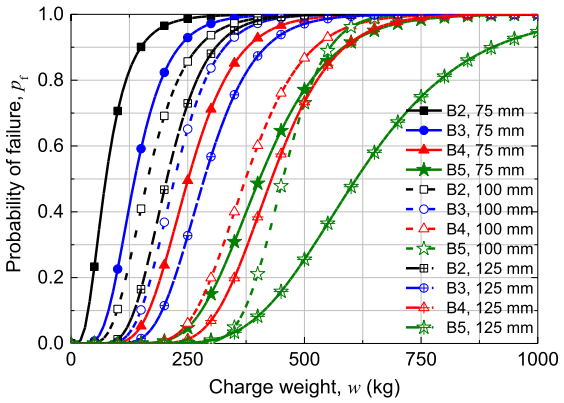

Fig. 14. Fragility curves of the RC wall panels members under free airburst scenario considering charge weight as intensity measure parameter.

Table 6
Difference in charge weight required to cause 50% failure probability.

Panel size	Damage levels	Charge weight for surface-burst (kg)	Charge weight for free airburst (kg)	% Change in charge weight
75 mm	B2	58	74.11	27.77%
	B3	82.71	136.83	65.43%
	B4	134.51	250.25	86.04%
	B5	223.45	405.62	81.52%
100 mm	B2	77.95	163.91	110.27%
	B3	114.599	221.54	93.31%
	B4	211.97	374.26	76.56%
	B5	291.50	452.65	55.28%
125 mm	B2	105.19	205.05	94.93%
	B3	165.91	285.277	71.94%
	B4	272.69	428.22	57.03%
	B5	368.96	612.29	65.95%

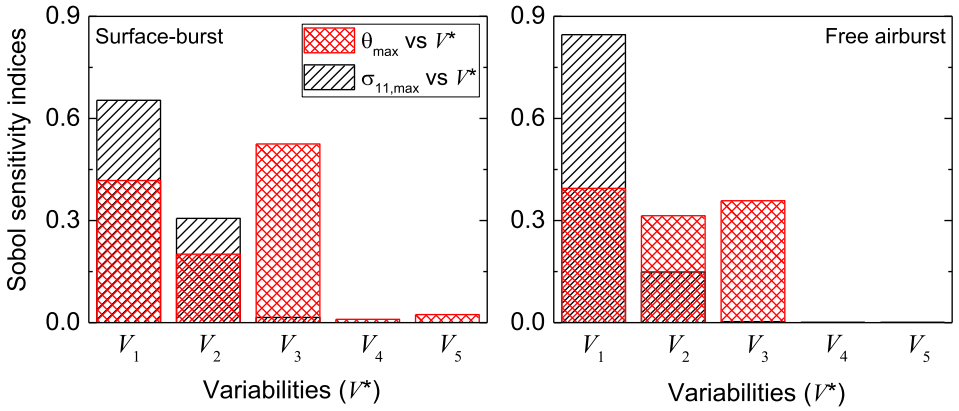

Fig. 15. Sensitivity analyses of the RC wall panels under surface-burst and free airburst scenarios.

parameters have significant influence (>95%) on the rotation response of the RC walls. Variabilities in material properties such as, strength of concrete and steel, and axial live load in terms of eccentric load have minimal effect on the stochasticity of the blast response. On the other hand, the stress response is not only influenced by the loading intensity parameters, but also influenced by strength of concrete material. For both types of blast scenarios, the concrete strength has significant influence, ~ 52% and ~36% respectively on the stress response of the RC wall panels. Hence, charge weight, standoff distance, and strength of concrete material are recommended to be crucial parameters for design of blast-resistant structures.

7. Conclusions

Herein, a stochastic approach is employed to compute probability of failure for RC wall panels under surface-burst and free airburst

scenarios. Uncertainties in the system are considered in structural capacity in terms of material strength, axial live load in terms of eccentric loading, and blast intensity in terms of charge weight and standoff distance to study the probabilistic blast response for the RC walls. Finally, sensitivity analysis is performed to observe the influence of random input variables on the distribution of output response. Hence, considering this investigation, the major conclusions drawn are as follows:

1. Based on the sensitivity analysis performed, charge weight, standoff distance, and strength of concrete material are recommended to be crucial parameters for design of blast-resistant structures.
2. The prescriptive design approach utilizing the deterministic method may overestimate the design values, which may not essentially evaluate the structural response accurately. The extent of uncertainty induced in the system has significant influence in the response of the wall panels under blast loading scenarios. In this regard, it is recommended to introduce more rational stochastic approach in design guidelines and standards for assessing new and retrofit existing structures under scenario-based blast loads.
3. Based on the fragility functions obtained, the increase in probability of failure is relatively more with standoff distance as the intensity measure (IM) parameter, as compared to that with the charge weight as the IM parameter.
4. The residual response, being an indicator of the degree of damage induced in a structural member, shows that the wall panels under surface-burst scenario have induced ~4.4 to 9.7 times the damage as compared to the free airburst scenario. Hence, the design guidelines should rationally address the differences in damaging consequences should the structure be designed under surface-burst scenario as compared to free airburst scenario.
5. Finally, it is crucial to consider the type of blast exposure in order to have a rational design for protection of structures against accidental blast loads. Moreover, based on the currently considered scenario of intensity of blast, standoff distance, exposure type, and performance level required by the user, it is recommended to specify minimum wall panel of thickness 100 mm, and especially 125 mm to counter the effects of extreme blast loadings.

Declaration of Competing Interest

The authors declare that they have no known competing financial interests or personal relationships that could have appeared to influence the work reported in this paper.

References

[1] ABAQUS/ Standard User's Manual, Version 6.14, Dassault Systemes, Simulia Corporation, Province, Rhode Island (RI), USA.
[2] A. Abbas, M. Adil, N. Ahmad, I. Ahmad, Behavior of reinforced concrete sandwiched panels (RCSPs) under blast load, Eng. Struct. 181 (15) (2019) 476–490.
[3] S.A. Akers, D.D. Rickman, J.Q. Ehrgott Jr., T.W. Shelton, Explosive breaching of reinforced concrete walls: experimental efforts and numerical simulations, American Concrete Institute, ACI Special Publication 281 (2010) 249–261.
[4] Y. Al-Salloum, T. Almusallam, S.M. Ibrahim, H. Abbas, S. Alsayed, Rate dependent behavior and modeling of concrete based on SHPB experiments, Cem. Concr. Compos. 55 (2015) 34–44.
[5] D. Asprone, E. Cadoni, A. Prota, Experimental analysis on tensile dynamic behavior of existing concrete under high strain rates, ACI Struct. J. 106 (1) (2009) 106–113.
[6] H. Baji, H.R. Ronagh, R.E. Melchers, Reliability of ductility requirements in concrete design codes, Struct. Saf. 62 (2016) 76–87.
[7] R.K. Chaudhary, S. Mishra, T. Chakraborty, V. Matsagar, Vulnerability analysis of tunnel linings under blast loading, Int. J. Protective Struct. 10 (1) (2019) 73–94.
[8] J.-H. Choi, S.-J. Choi, J.-H.J. Kim, K.-N. Hong, Evaluation of blast resistance and failure behavior of prestressed concrete under blast loading, Constr. Build. Mater. 173 (2018) 550–572.
[9] D. Cormie, G. Mays, P. Smith, "Blast effects on buildings", Thomas Telford Publishing, 2nd Edition, London, UK, 2009.
[10] B. Ellingwood, C. Culver, Analysis of live loads in office buildings, J. Struct. Div. (ASCE) 103 (8) (1977) 1551–1560.
[11] B. Ellingwood, T.V. Galambos, J.G. MacGregor, C.A. Cornell, "Development of a probability-based load criterion for American National Standard A58 - Building code requirement for minimum design loads in buildings and other structures", *Special Publication* 577, Department of Commerce, National Bureau of Standards, Washington D.C, USA, U.S, 1980.
[12] A.E. El-Sisi, A. Saucier, H.A. Salim, J.M. Hoemann, Experimental and numerical evaluation of reinforced concrete walls retrofit systems for blast mitigation, J. Perform. Constr. Facil (ASCE) 33 (2) (2019) 04018113.
[13] FEMA P-58 (2012), "Next-generation methodology for seismic performance assessment of buildings", Applied Technology Council (ATC), Federal Emergency Management Agency (FEMA), Washington D.C., USA.
[14] M.D. Goel, V.A. Matsagar, Blast-resistant design of structures, Practice Periodical on Structural Design and Construction (ASCE), 19(2), Article Number 04014007, 2014.
[15] M.D. Goel, V.A. Matsagar, A.K. Gupta, Blast resistance of stiffened sandwich panels with aluminum cenosphere syntactic foam, Int. J. Impact Eng. 77 (2015) 134–146.
[16] M.J. Gombeda, C.J. Naito, S.E. Quiel, Performance-based framework for evaluating the flexural response of precast concrete wall panels to blast loading, Eng. Struct. 168 (1) (2018) 473–486.
[17] A. Goswami, S.D. Adhikary, Retrofitting materials for enhanced blast performance of Structures: recent advancement and challenges ahead, Constr. Build. Mater. 204 (2019) 224–243.
[18] X. Huang, H. Bao, Y. Hao, H. Hao, Damage assessment of two-way RC slab subjected to blast load using mode approximation approach, Int. J. Struct. Stab. Dyn. 17 (1) (2017). Article Number 1750013.
[19] IS 456 (2000), "Plain and reinforced concrete - code of practice", Bureau of Indian Standards (BIS), New Delhi, India.
[20] IS 875 - Part 2 (1987), "Code of practice for design loads (other than earthquake) for buildings and structures: imposed loads", Bureau of Indian Standards (BIS), New Delhi, India.
[21] E. Jacques, A. Lloyd, M. Saatcioglu, Predicting reinforced concrete response to blast loads, Can. J. Civ. Eng. 40 (5) (2013) 427–444.
[22] S. Jain, R. Tiwari, T. Chakraborty, V.A. Matsagar, Dynamic response of reinforced concrete wall under blast loading, Indian Concr. J. 89 (8) (2015) 27–41.
[23] D. Kelliher, K. Sutton-Swaby, Stochastic representation of blast load damage in a reinforced concrete building, Struct. Saf. 34 (1) (2012) 407–417.
[24] S. Khan, S.K. Saha, V.A. Matsagar, B. Hoffmeister, Fragility of steel frame buildings under blast load, J. Perform. Constr. Facil (ASCE) 31 (4) (2017). Article Number 04017019.
[25] G.F. Kinney, K.J. Graham, Explosive shocks in air, 2nd ed., Springer, Berlin, Germany, 1985.
[26] T. Krauthammer, N. Bazeos, T.J. Holmquist, Modified SDOF analysis of RC box-type structures, J. Struct. Eng. (ASCE) 112 (4) (1986) 726–744.

[27] T. Krauthammer, S. Shahriar, H.M. Shanaa, Response of reinforced concrete elements to severe impulsive loads, J. Struct. Eng. (ASCE) 116 (4) (1990) 1061–1079.
[28] A. Kumar, V. Matsagar, Blast fragility and sensitivity analyses of steel moment frames with plan irregularities, Int. J. Steel Struct. 18 (5) (2018) 1684–1698.
[29] A. Kumar, S.K. Saha, V.A. Matsagar, Stochastic response analysis of elastic and inelastic systems with uncertain parameters under random impulse loading, J. Sound Vib. 461 (2019), 114899.
[30] X. Lin, Y.X. Zhang, P.J. Hazell, Modelling the response of reinforced concrete panels under blast loading, Mater. Des. 56 (2014) 620–628.
[31] J. Liu, C. Wu, C. Li, W. Dong, Y. Su, J. Li, N. Cui, F. Zeng, L. Dai, Q. Meng, J. Pang, Blast testing of high performance geopolymer composite walls reinforced with steel wire mesh and aluminum foam, Constr. Build. Mater. 197 (2019) 533–547.
[32] H.Y. Low, H. Hao, Reliability analysis of reinforced concrete slabs under explosive loading, Struct. Saf. 23 (2) (2001) 157–178.
[33] D. Lu, G. Wang, X. Du, A nonlinear dynamic uniaxial strength criterion that considers the ultimate dynamic strength of concrete, Int. J. Impact Eng. 103 (2017) 124–137.
[34] C.M. Morison, Dynamic response of walls and slabs by single-degree-of-freedom analysis - A critical review and revision, Int. J. Impact Eng. 32 (8) (2006) 1214–1247.
[35] M.D. Netherton, M.G. Stewart, Blast load variability and accuracy of blast load prediction models, Int. J. Protective Struct. 1 (4) (2010) 543–570.
[36] A.S. Nowak, M.M. Szerszen, Calibration of design code for buildings (ACI 318): part I-statistical models for resistance, ACI Struct. J. 100 (3) (2003) 377–438.
[37] P. Olmati, F. Petrini, K. Gkoumas, Fragility analysis for the performance-based design of cladding wall panels subjected to blast load, Eng. Struct. 78 (2014) 112–120.
[38] Y.G. Pan, A.J. Watson, Interaction between concrete cladding panels and fixings under blast loading, Cem. Concr. Compos. 18 (5) (1996) 323–332.
[39] C.P. Pantelides, T.T. Garfield, W.D. Richins, T.K. Larson, J.E. Blakeley, Reinforced concrete and fiber reinforced concrete panels subjected to blast detonations and post-blast static tests, Eng. Struct. 76 (2014) 24–33.
[40] F. Parisi, Blast fragility and performance-based pressure-impulse diagrams of European reinforced concrete columns, Eng. Struct. 103 (2015) 285–297.
[41] PDC-TR-06-08 (2008), "Single degree of freedom structural response limits for antiterrorism design", US Army Corps of Engineers Protective Design Center.
[42] T. Roy, P. Agarwal, Comparison of damage index and fragility curve of RC structure using different Indian standard codes, Adv. Struct. Eng., Springer 3 (2015) 2551–2563, https://doi.org/10.1007/978-81-322-2187-6_197.
[43] T. Roy, V. Matsagar, Fire fragility of reinforced concrete panels under compressive in-plane and transverse out-of-plane loads, Fire Saf. J. 113 (2020), 102976.
[44] T. Roy, V. Matsagar, Probabilistic assessment of steel buildings installed with passive control devices under multi-hazard scenario of earthquake and wind, Struct. Saf. 85 (2020), 101955.
[45] T. Roy, V. Matsagar, Mechanics of damage in reinforced concrete member under post-blast fire scenario, Structures 31 (2021) 740–760, https://doi.org/10.1016/j.istruc.2021.02.005.
[46] P. Russo, F. Parisi, Risk-targeted safety distance of reinforced concrete buildings from natural-gas transmission pipelines, Reliab. Eng. Syst. Saf. 148 (2016) 57–66.
[47] A. Saltelli, I.M. Sobol, About the use of rank transformation in sensitivity analysis of model output, Reliab. Eng. Syst. Saf. 50 (3) (1995) 225–239.
[48] Y. Shi, M.G. Stewart, Damage and risk assessment for reinforced concrete wall panels subjected to explosive blast loading, Int. J. Impact Eng. 85 (10) (2015) 5–19.
[49] M. Shinozuka, M.Q. Feng, J. Lee, T. Naganuma, Statistical analysis of fragility curves, J. Eng. Mech. (ASCE) 126 (12) (2000) 1224–1231.
[50] P.F. Silva, B. Lu, Improving the blast resistance capacity of RC slabs with innovative composite materials, Compos. B: Eng. 38 (5–6) (2007) 523–534.
[51] P.F. Silva, B. Lu, Blast resistance capacity of reinforced concrete slabs, J. Struct. Eng. (ASCE) 135 (6) (2009) 708–716.
[52] I.M. Sobol, Global sensitivity indices for nonlinear mathematical models and their Monte Carlo estimates, Math. Comput. Simul 55 (1–3) (2001) 271–280.
[53] P. Soroushian, K. Choi, Steel mechanical properties at different strain rates, J. Struct. Eng. 113 (4) (1987) 663–672.
[54] M.G. Stewart, Reliability-based load factor design model for explosive blast loading, Struct. Saf. 71 (2018) 13–23.
[55] M.G. Stewart, M.D. Netherton, Y. Shi, M. Grant, Probabilistic terrorism risk assessment and risk acceptability for infrastructure protection, Aust. J. Struct. Eng. 13 (1) (2012) A001.
[56] D.-K. Thai, S.-E. Kim, Numerical investigation of the damage of RC members subjected to blast loading, Eng. Fail. Anal. 92 (2018) 350–367.
[57] Y.-K. Tsai, T. Krauthammer, Energy based load-impulse diagrams with multiple failure modes for blast-loaded reinforced concrete structural elements, Eng. Fail. Anal. 104 (2019) 830–843.
[58] UFC 3-340-02, "Design of structures to resist the effects of accidental explosions", US Department of Defense, Washington D.C., USA, 2008.
[59] UFC 4-010-01, "Minimum antiterrorism standards for buildings", US Department of Defense, Washington D.C., USA, 2012.
[60] B. Wang, P. Wang, Y. Chen, J. Zhou, X. Kong, H. Wu, H. Fan, F. Jin, Blast responses of CFRP strengthened autoclaved aerated cellular concrete panels, Constr. Build. Mater. 157 (2017) 226–236.
[61] W. Wang, C. Wu, J. Li, Numerical simulation of hybrid FRP-concrete-steel double-skin tubular columns under close-range blast loading, J. Compos. Constr. (ASCE) 22 (5) (2018). Article Number 04018036.
[62] J. Wu, Y. Zhou, R. Zhang, C. Liu, Z. Zhang, Numerical simulation of reinforced concrete slab subjected to blast loading and the structural damage assessment, Eng. Fail. Anal. 118 (2020), 104926.
[63] K. Xu, Y. Lu, Numerical simulation study of spallation in reinforced concrete plates subjected to blast loading, Comput. Struct. 84 (5–6) (2006) 431–438.
[64] S. Yao, D. Zhang, X. Chen, F. Lu, W. Wang, Experimental and numerical study on the dynamic response of RC slabs under blast loading, Eng. Fail. Anal. 66 (2016) 120–129.
[65] R. Yu, L. Chen, Q. Fang, Y. Huan, An improved nonlinear analytical approach to generate fragility curves of reinforced concrete columns subjected to blast loads, Adv. Struct. Eng. 21 (3) (2018) 396–414.
[66] X.H. Yu, D.G. Lu, K. Qian, B. Li, Uncertainty and sensitivity analysis of reinforced concrete frame structures subjected to column loss, J. Perform. Constr. Facil (ASCE) 31 (1) (2017). Article Number 04016069.
[67] X.Q. Zhou, H. Hao, Modelling of compressive behavior of concrete-like materials at high strain rate, Int. J. Solids Struct. 45 (17) (2008) 4648–4661.